Journal of Chromatography A, 1236 (2012) 105–114

Contents lists available at SciVerse ScienceDirect

Journal of Chromatography A

journal homepage: www.elsevier.com/locate/chroma

Kinetic performance of narrow-bore columns on a micro-system for high performance liquid chromatography

Fabrice Gritti, Georges Guiochon*

Department of Chemistry, University of Tennessee, Knoxville, TN 37996-1600, USA

ARTICLE INFO

Article history:
Received 4 December 2011
Received in revised form 28 February 2012
Accepted 1 March 2012
Available online 14 March 2012

Keywords:
Column technology
Core–shell particles
Instrument band broadening
μHPLC
Halo-C_{18}

ABSTRACT

The kinetic performance of 0.5 mm × 50 mm columns packed with 2.7 μm Halo-C_{18} core–shell particles and 3 μm EP-120-C_{18} fully porous particles fitted on an Eksigent LC-Express Ultra μHPLC system were measured. The instrument contribution to band broadening was obtained by directly connecting the injection valve and the detector cell with a short, narrow PEEKSIL tube. The connections between the column and the connecting tubes, the column endfittings and its frits contribute to band spreading and are responsible for a significant rear peak tailing, even for retained compounds, resulting in a significant loss of efficiency. Our results show that the μHPLC system could outperform the current VHPLC systems using 2.1 mm I.D. columns packed with 1.7 μm particles if it were using 0.5 mm I.D. columns packed with 1 μm particles, if it could operate at a few kbar pressure drop, and if the sum of the contributions of the instrument, column endfittings and the column frits to band dispersion were three times smaller than it is at present.

1. Introduction

Over the last ten years, chromatographic column technology has evolved considerably, due to the successful development of sub 2 μm particles [1] and sub 3 μm core–shell particles [2–11] with which columns are now packed. Sub 2 μm particles provide low permeability columns that have high optimum velocities. Their use requires resorting to very high inlet pressures and to develop very high pressure liquid chromatography (VHPLC) technique and instruments able to operate under pressures exceeding 1000 bar and allowing a significant decrease in the column size [12]. The volumes of bands eluted from short columns packed with sub 2 μm particles are smaller than were those of bands eluted from traditional columns. Therefore, modern instruments must have lower extra-column band broadening contributions than had the conventional instruments of the late last century. They do provide low extra-column band dispersion but cannot avoid to cause a certain loss of efficiency of modern columns [13–15]. This efficiency loss can somehow be minimized by increasing the retention of critical compounds to generate an overall peak variance sufficiently larger than the system variance.

Furthermore, the combination of the high flow rates percolating through 2.1 mm I.D. columns packed with sub-2 μm particles and the high pressure gradients that are required to provide these flow rates generate important friction heat, the dispersion of which causes significant thermal gradients across the column, with detrimental consequences for the column efficiency [16]. Proper attention is required to achieve high performance in analytical separations, e.g., by running the columns under nearly adiabatic conditions, which minimizes the radial temperature gradients [17,19–22]. The use of narrower columns also reduces the importance of heat effects, since the flow rates becoming smaller, less heat power is generated per unit column length at constant pressure gradient, the radial temperature gradients are decreased and they are relaxed faster due to the narrower radius. In practice, heat friction effects are rarely negligible with 2.1 mm I.D. columns [21,22] and this is particularly true when low heat conductivity eluents (e.g., acetonitrile) are used and columns are packed with fully porous particles [23,24,16].

The heat problem can be considerably alleviated if the column diameter is reduced to 0.3 or 0.5 mm. New μHPLC systems have been produced for this purpose. However, shrinking the column diameter causes a severe reduction of the variance of eluted bands, which in turn demands drastic changes in the instrument design. Combining narrower connection tubes, low volume injection valves, smaller detector cell volume, and completely redesigning the injection system resulted in the design of μHPLC instruments having an extra-column variance contribution at least four times smaller than the variance of the bands eluted from 0.5 mm × 50 mm columns packed with sub-3 μm particles with retention factors larger than 2. The overall (system +column) or apparent efficiency should then exceed 80% of the intrinsic column efficiency. For example, with a moderate retention factor $k = 2$ and a plate height of 6.5 μm, the overall peak variance of a

* Corresponding author. Fax: +1 865 974 2667.
E-mail address: guiochon@utk.edu (G. Guiochon).

0021-9673/$ – see front matter © 2012 Elsevier B.V. All rights reserved.
doi:10.1016/j.chroma.2012.03.007

Nomenclature

Roman letters

d_p	average particle diameter (m)
D_m	bulk molecular diffusion coefficient (m^2/s)
D_p	particle diffusivity (m^2/s)
F_v	flow rate (m^3/s)
h	reduced plate height
k	retention factor
k_1	zone retention factor.
K_c	Kozeny–Carman constant.
k_0	specific permeability (m^2).
L	column length (m).
N	column efficiency
P_f	heat friction power per unit length of the column (W/m)
ΔP	column pressure drop (Pa)
r_c	column inner radius (m)
r_{cap}	capillary radius (m)
T	temperature (K)
t_d	critical diffusion time (s)
u	interstitial linear velocity (m/s)
u_{opt}	interstitial linear velocity at the optimum column efficiency (m/s)
V_{inj}	injection volume (m^3)

Greek letters

α_p	isobaric expansion coefficient (K^{-1})
ϵ_e	external column porosity
ϵ_t	total column porosity
η	eluent viscosity (Pa s)
ν	reduced interstitial linear velocity
λ_p	effective heat conductivity of the packed bed (W/m/K)
$\sigma^2_{v,column}$	volume variance contribution of the column (m^6)
$\sigma^2_{v,system}$	volume variance contribution of the HPLC system (m^6)
$\sigma^2_{v,system,disp}$	volume variance contribution of the HPLC system for a δ-Dirac injection (m^6)
$\sigma^2_{v,system,inj}$	volume variance contribution of the injection volume (m^6)

0.5 mm × 50 mm column is 0.04 μL², requiring an extra-column peak variance smaller than 0.01 μL². Therefore, current HPLC instruments cannot operate such a narrow-bore column since their band variance exceeds 1 μL². Finally, a subsidiary advantage of μHPLC systems is the reduction of eluent consumption by at least one order of magnitude.

The limitation of the μHPLC equipments currently available is a maximum back pressure of only 700 bar. Consider a 0.5 mm × 50 mm column packed with 1.5 μm particles (permeability around 2.2×10^{-15} m^2). Its optimum interstitial linear velocity for the elution of small molecules (diffusion coefficient around 1.5×10^{-5} cm^2/s) would be of the order of $10 \times D_m \times d_p^{-1}$ or 1 cm/s. Even with a low viscosity eluent, $\eta = 0.5$ cP, the column back pressure should be as high as 1150 bar. So, these instruments cannot be used for optimum/fast analyses of low molecular weight compounds, unless they are packed with particles larger than 2.0 μm. In contrast, they could be most useful for the analyses of high molecular weight compounds such as proteins (e.g., $D_m \simeq 10^{-6}$ cm^2/s or smaller) for which the optimum linear velocity should be around 0.07 cm/s (optimum flow rate of 3 μL/min), requiring a back pressure of only 75 bar. In fact, μHPLC systems allowing flow rates between 10 and 60 μL/min at a maximum inlet pressure of 700 bar are well suited for the analysis of low molecular weight compounds, using 0.5 mm × 50 mm columns packed with 2–3 μm particles. Their optimal flow rates is between 25 and 35 μL/min for pressure drops between 140 and 470 bar.

The intrinsic efficiency of commercial narrow-bore columns depends on their inner diameter. For instance, 2.1 mm I.D. columns packed with core–shell particles exhibit efficiencies 35% lower than that of 4.6 mm I.D. columns packed with the same material [25]. No detailed study of the efficiencies of 1 mm or narrower columns packed with fully or superficially porous particles has yet been published. Serious doubts remain as to whether one can pack satisfactorily columns narrower than 1 mm. In practice, the apparent efficiency of columns derived from uncorrected chromatograms seems to decrease with decreasing column diameter, which is certainly explained, at least in part, with the difficulties in estimating and reducing the band broadening effects of the system/column connections and of the column endfittings and frits that potentially decrease the efficiency of narrow-bore columns. Little is said in the literature on the importance of the peak variances of sub-1 mm I.D. columns due to these necessary ancillary devices that are of primary importance in the design of these instruments.

The goal of this work was to assess the intrinsic performance of 0.5 mm I.D. columns packed with 3 μm fully porous particles and 2.7 μm superficially porous particles and to measure the band broadening contributions of a commercial μHPLC system in the elution of small molecules. The flow rates range between 10 and 60 μL/min. The comparison of the efficiencies of 0.5 mm I.D. columns and of 2.1 mm and 4.6 mm I.D. columns packed with 2.7 μm Halo particles permits an assessment of the speed-resolution performance of conventional HPLC and μHPLC systems.

2. Theory

2.1. Definitions and basic chromatographic relationships

The reduced interstitial linear velocity, ν, is written:

$$\nu = \frac{u d_p}{D_m} \tag{1}$$

where d_p is the mean particle diameter, D_m is the bulk diffusion coefficient, and u is the average interstitial linear velocity along the column given by:

$$u = \frac{F_v}{\epsilon_e \pi r_c^2} \tag{2}$$

where F_v is the flow rate and r_c is the inner column radius.

The optimal reduced velocity, ν_{opt}, is the reduced velocity at the minimum of the reduced HETP curve. In well packed columns, e.g. in the absence of significant trans-column/long-range velocity biases, we usually expect ν_{opt} to be approximately 10. Therefore, the expected optimal interstitial linear velocity, u_{opt}, should be about

$$u_{opt} = \frac{10 D_m}{d_p} \tag{3}$$

The specific permeability, k_0, is given by [26]:

$$k_0 = \frac{\epsilon_e^3 d_p^2}{(1-\epsilon_e)^2 K_c} \tag{4}$$

where ϵ_e is the external porosity of the packed bed and K_c is the Kozeny–Carman constant, which is considered to be equal to 180 for packed spherical particles. Therefore, the column back pressure, ΔP, at the optimum linear velocity is given by:

$$\Delta P = \frac{\eta L}{k_0} u_{opt} \tag{5}$$

where η is the viscosity of the eluent, and L is the column length.

The volume peak variance, $\sigma^2_{v,column}$, of a retained compound (retention factor k) caused by the sole contribution of the chromatographic column is:

$$\sigma^2_{v,column} = \frac{\epsilon_t^2 \pi^2 r_c^4 L^2}{N}(1+k)^2 \quad (6)$$

where ϵ_t is the total porosity of the chromatographic column and N its efficiency.

The total observed peak variance, $\sigma^2_{v,column}$, is

$$\sigma^2_{v,column} = \sigma^2_{v,column} + \sigma^2_{v,system} \quad (7)$$

where $\sigma^2_{v,system}$ is the volume peak variance contributed to by the instrument only. It is the sum of the contributions of the dispersion of a δ-Dirac function through the system, $\sigma^2_{v,system,disp}$, and that of the injection volume, $\sigma^2_{v,system,inj}$. Therefore,

$$\sigma^2_{v,system} = \sigma^2_{v,system,disp} + \sigma^2_{v,system,inj} = \sigma^2_{v,system,disp} + \frac{V^2_{inj}}{12} \quad (8)$$

where V_{inj} is the injected sample volume. The heat power produced per unit length of column, P_f, is [27,28,21]:

$$P_f = \epsilon_e u \pi r_c^2 \times \frac{\Delta P}{L} \quad (9)$$

The amplitude of the radial temperature gradient, ΔT, across the column diameter under steady-state conditions is [27]:

$$\Delta T = (1 + \overline{\alpha_p T})\epsilon_e u r_c^2 \frac{\Delta P}{4\lambda_p L} \quad (10)$$

where α_p is the isobaric expansion coefficient of the eluent, T is the average temperature across the column diameter, $\overline{\alpha_p T}$ is the average values over the column volume of the product of these two physical properties, and λ_p is the effective heat conductivity of the packed bed immersed in the eluent. Note that, in practice, radial temperature gradients are not fully developed and are coupled with axial temperature gradients. Eq. 10 overestimates the true value of the amplitude of the radial temperature gradients but it indicates the order of magnitude of the effect to be expected.

3. Experimental

3.1. Chemicals

The mobile phase was a mixture of acetonitrile and water (65/35, v/v). Both solvents were HPLC grade from Fisher Scientific (Fair Lawn, NJ, USA). They were filtered before use on a surfactant-free cellulose acetate filter membrane, 0.2 μm pore size (Suwannee, GA, USA). The sample naphthalene was purchased from Fisher Scientific, with a minimum purity of 99%.

3.2. Apparatus

The ExpressLC®-Ultra μHPLC system used in this work was loaned by its manufacturer, Eksigent (Dublin, CA, USA). It includes a binary micro-pump system and an automatic auto-sampler. The available flow-rate range is between 10 and 60 μL/min. The accuracy of the flow rate is 1%, assessed by filling a 100 μL calibration capillary tube during 4 min, at a flow rate targeted of 25 μL/min. The injection system consists of an injection loop (500 nL) directly connected to a micro selection valve 6 ports/2 positions (inject and loading) (65 nL). The shortest switching time, t_{switch}, between the load and inject positions is 150 ms. Therefore, the injected volume cannot be smaller than the product of the flow rate by 0.150 ms. For instance, at the maximum flow rate of 60 μL/min, the minimum injected volume is 150 nL. Also, for each injection, the injection loop

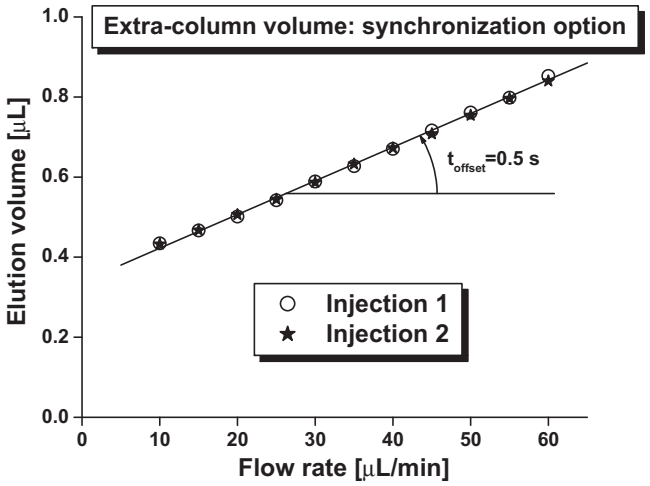

Fig. 1. Plot of the product of the first moment, $\mu_{1,system}$, of the system peak profile and the flow rate as a function of the flow rate. Injection mode: synchronization, partial loop, 160 nL injected. Note the significant offset time of half a second between the zero time and the actuation of the injection valve.

is completely filled and the volume of sample drawn into the 100 μL syringe and dispensed into the needle seat capillary is 15 μL. The sample syringe and needle seat capillary are washed thrice with pure acetonitrile before and after sample delivery, respectively. The instrument is also equipped with a compartment oven and a single array UV–VIS detection system. The volume of the detection cell is 100 nL. The highest sampling rate is 100 Hz. The whole μHPLC system is controlled by the Eksigent software.

In the absence of a column, when the extra-column peak variances of naphthalene were measured, the sample trajectory in the equipment involves their successive passage through

- One end of the 500 nL injection loop attached to the injection needle (partial loop injection option was selected). The volume of sample drawn is necessarily larger than $F_v \times t_{switch}$ and smaller than 500 nL.
- The micro injection valve. The total volume of the grooves and the connection ports of the valve is 65 nL.
- One PEEKSIL connector capillaries (orange tubing), 150 mm long with 25 μm inner diameter. Its volume is 74 nL.
- A small volume detector cell, with a total volume 150 nL and a 5 mm optical path length. The volume of the flow cell is 100 nL. The volumes of the inlet and outlet connectors are 25 nL each.

Fig. 1 shows how the extra-column volume was measured. A 160 nL sample plug was injected at 10, 15, 20, 25, 30, 35, 40, 45, 50, 55, and 60 μL/min. The product of the first moment (measured by peak integration) by the flow rate was plotted as a function of the flow rate. The obvious positive slope means that the zero in the output file was set before the valves physically switched from the loading to the inject position. This offset time (or the slope of the linear plot) was measured at 0.5 s. The extrapolation of the linear plot to a zero flow rate gives a volume of 334 nL, suggesting that the extra-column volume corrected for the injection volume is equal to 334 − (160/2) = 254 nL. By difference, we also estimate the total volume of the three connections (injection loop-valve, valve-PEEKSIL and PEEKSIL-detector) at 254 − 65 − 74 − 25 − 50 nL = 40 nL.

In the presence of a chromatographic column, the 15 cm long PEEKSIL tube was replaced with a 10 cm long PEEKSIL tube (25 μm I.D. before the column) and a 7 cm long PEEKSIL filter capillary (25 μm I.D. after the column).

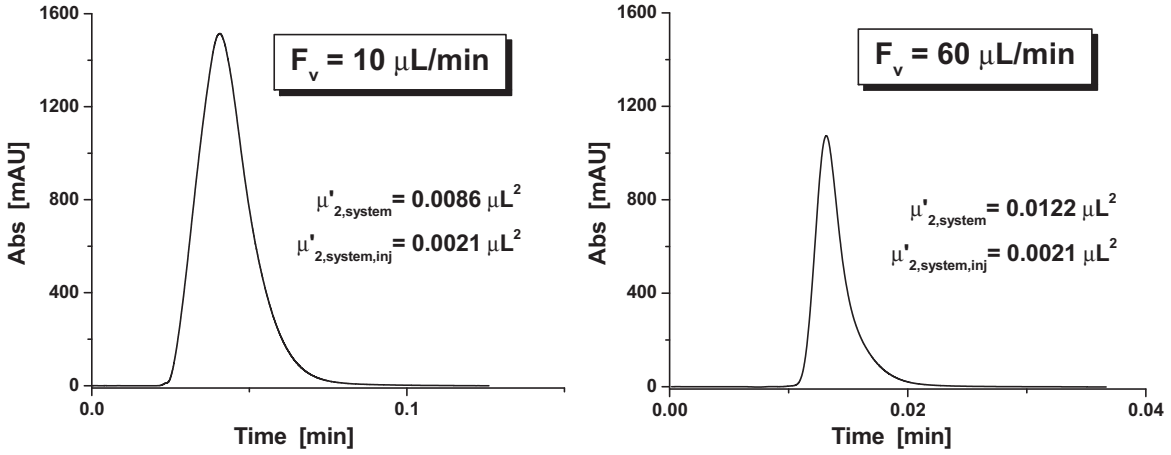

Fig. 2. Example of system band profiles of naphthalene recorded with the LC-Express Ultra system. Eluent: acetonitrile/water, 65/35, v/v. T = 295 K. The injection valve and the detector cell were connected with a 25 μm ×150 mm PEEKSIL tube. The injection volume was 160 nL. The signal sampling rate was 100 Hz. Left graph: F_v = 10 μL/min. Right graph: F_v = 60 μL/min. Note that the contribution of the injected sample plug ($V_{inj}^2/12$) accounts for 24% and 17% of the total band variance.

3.3. Columns

Three 0.5 mm × 50 mm columns were provided by the manufacturer (Eksigent, Dublin, CA, USA). The two Halo columns (1 and 2, serial numbers 050411-001 and 031411-12236-004) were packed according to a proprietary process with the same batch of 2.7 μm Halo-C_{18} 90 Å shell particles from Advanced Material Technology (Wilmington, DE, USA). The third column was packed with 3 μm Prontosil-C_{18}-EP 120 Å fully porous particles (Bishoff Chromatography, Leonberg, Germany, serial number 071610-14-007). The Halo columns 1 and 2 differ by the nature of their inlet and outlet proprietary endfittings. The endfittings of the column packed with the fully porous material are the same as those of the Halo column 2.

During all the HETP sequence runs, the columns were installed on the LC-Express μHPLC instrument and left under still air conditions at ambient temperature. They were protected from air convection by a door that covers the whole front of the instrument, including the injection port, the connecting tubes, and the detector.

3.3.1. HETP measurement

The HETPs of naphthalene on all three columns were acquired with the same sequence of flow rates. The sampling rate was set at 100 Hz for all flow rates. The volume injected was fixed at 160 nL from the partial loop injection mode. The temperature was set by the laboratory air-conditioner at 297 ± 1 K.

The HETP data were all measured by the numerical integration method and corrected to take into account peak tailing (or fronting) and instrument broadening. This method (described in detail in [29]) has the advantage of revealing any packing defect at the scale of the column diameter or, at least, at that of the long distances across which concentration gradients cannot be relaxed during sample migration. Also, it can reveal poorly designed connections between the system and the column and/or inlet and outlet frits. Nevertheless, this method is less precise than the conventional half-height peak width. All the details for the measurement of the HETP data and their accuracy are given elsewhere [29–31]. This method is very accurate but its precision is only around 10% for moderately retained compounds.

The diffusion coefficient of naphthalene at 295 K in the mixture of acetonitrile and water (65/35, v/v) used is $D_m = 1.46 \times 10^{-5}$ cm^2/s, as previously measured [32].

4. Results and discussion

This work is divided into four parts. In the first part, we report on the impact of the LC-Express Ultra μHPLC system on the band dispersion by placing a 25 μm ×150 mm PEEKSIL capillary between the injection valve and the detection cell. We compare it to that of a μHPLC system in the similar flow rate range, between 10 and 60 μL/min. In the second part, we report on measurements of the performance of 0.5 mm × 50 mm columns packed with core–shell (2.7 μm Halo-C_{18}) and fully porous (3 μm Prontosil-C_{18}-EP-120) particles and discuss these results. In the third part, we compare them to those provided by 2.1 mm and 4.6 mm I.D. columns packed with similar packing materials. Finally, we investigate the role of μHPLC in the analysis of small molecules using columns packed with 1 μm particles.

4.1. Extra-column contribution

The contribution of the LC-Express Ultra μHPLC system to the observed band dispersion was measured by connecting directly the injection valve and the detection cell with a 25 μm ×150 mm PEEKSIL tube. The range of flow rate was from 10 to 60 μL/min. The injection was set at 160 nL. Fig. 2A and B shows two examples of extra-column band profiles recorded with naphthalene at flow rates of 10 and 60 μL.

The volume variance of the eluted peaks of naphthalene are around 0.01 μL^2. Fig. 3 shows the variation of the second central moment, μ_2', with increasing flow rate. After correction for the width of the injected plug, it increases, from 0.0065 to 0.0101 μL^2, for with increasing flow rate from 10 to 60 μL/min. This shows that the extra-column peak variance is accounted for by the non-ideal behavior of the injection process and the passage of the band through the complex channels of the instrument. Had the injection been ideal, the band variance would be only $0.16^2/12 = 0.0021$ μL^2.

For comparison, on the 1290 Infinity VHPLC system, the extra-column peak variance of a 0.5 μL naphthalene sample, in the same eluent (acetonitrile/water, 65/35, v/v), and at the same temperature (295 K) increases linearly from 0.29 to 1.90 μL^2 in a comparable flow rate range [14]. The 1290 Infinity system was equipped with a needle seat capillary (115 μm ×150 mm), a 1.2 μL injection valve, a 115 μ ×220 mm connecting tube, a zero dead volume (ZDV) union connector, a second 115 μm ×220 mm connecting tube, and a 0.8 μL detector cell. The total extra-column volume of the HPLC 1290 Infinity system was 8.5 μL while that of the μHPLC system is

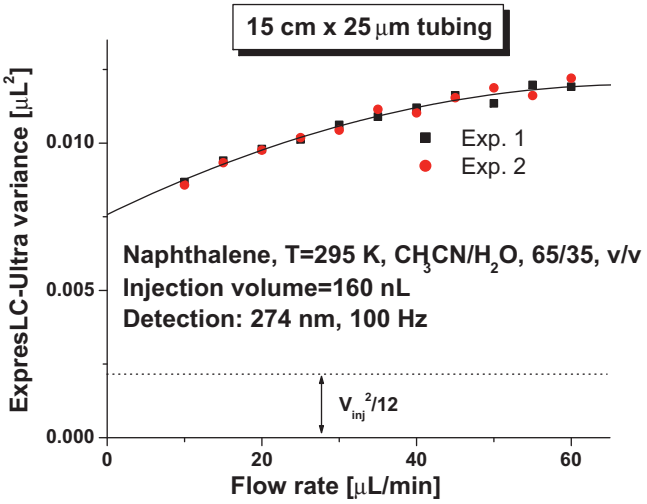

Fig. 3. Plot of the second central moment of naphthalene, $\mu'_{2,system}$, recorded in the absence of a chromatographic column with the LC-Express Ultra μHPLC system as a function of the flow rate. Injection mode: synchronization, partial loop, 160 nL injected. Eluent: acetonitrile/water, 65/35, v/v. T = 295 K.

0.254 μL, about 30 times smaller. At flow rates of 10 and 60 μL/min, the variances of the 1290 HPLC system are about 50 and nearly 200 times larger than those of the μHPLC system, respectively.

The critical diffusion time, t_d, necessary for sample molecules to radially diffuse and be transferred from the fast velocity flow stream in the center of channels to the zero velocity flow stream (no-slip condition, e.g. the eluent in contact to the wall of the tube is stagnant) at the wall of the tube is given by:

$$t_d = \frac{r_{cap}^2}{4D_m} \tag{11}$$

where r_{cap} is the capillary diameter.

Numerical applications of Eq. 11 with r_{cap} = 60 μm and $D_m = 1.5 \times 10^{-5}$ cm²/s gives t_d = 0.6 s. But the average residence time of naphthalene along the 1290 Infinity system was 48 and 8 s at 10 and 60 μL/min, respectively. These residence times are at least 13 times larger than the critical diffusion time. Similarly, with the LC-Express Ultra μHPLC system (r_{cap} = 12.5 μm), t_d = 0.026 s and the average residence times at 10 and 60 μL are 2.1 and 0.34 s, respectively. Therefore, the band broadening in the tubes and detection cell of either the 1290 Infinity system or the LC-Express Ultra μHPLC system is likely governed by the Aris–Taylor model of sample dispersion in a tube and the peak volume variance would increase linearly with increasing flow rate according to [33,34]:

$$\sigma^2_{v,system} = \frac{\pi}{24}\frac{F_v}{D_m} L r_c^4 \tag{12}$$

Additionally, Eq. 12 shows that the increasing rate of the volume variance with increasing flow rate is proportional to the product of the tube length (150 mm and 600 mm for the LC-Express Ultra μHPLC and the 1290 Infinity HPLC system, respectively) and to the fourth power of the tube radius (r_c = 12.5 and 57.5 μm, respectively). This simple theory predicts the ratio of the rates of variance increases of the two instruments to be around $4 \times 4.6^4 = 1790$. Actually, we measured a significantly smaller ratio, $(1.9 - 0.290/(0.0101 - 0.0065) = 447$, four times less. Most likely, the dispersion in the flow cell (100 nL) and in the injection valve (130 nL) of the μHPLC system are important and cannot be described by the simple Taylor-Aris model of dispersion that is valid along the 25 μm × 150 mm PEEKSIL tube (74 nL). According to the coupling between the diffusion (Taylor-Aris theory dispersion) and the flow dispersion mechanism along a cylindrical tubes, the variance is written [35]:

$$\sigma^2_{v,system} = \frac{\pi^2 r_c^4 L^2}{3 + (24\pi L D_m / F_v)} \tag{13}$$

For more details on the derivation of Eq. 13, we refer the reader to Ref. [35].

According to Eq. 13, the contributions of the PEEKSIL tube to the system peak variance are 0.00005 and 0.00027 μL² at flow rates of 10 and 60 μL/min, respectively, whereas we measured total system contributions of 0.00650–0.01010 μL². Accordingly, band dispersion through the 25 μm × 150 mm connecting tube accounts for only 0.8 and 2.7% of the total system peak variance at these flow rates. In contrast, with the vHPLC system (r_c = 57.5 μm and L = 600 mm), we would expect system peak variances of 0.095 and 0.548 μL². These variances account for as much as 33% and 29% or the instrument variance, respectively. This explains why the theoretical ratio, 1790, of the rates of variance increases in the two different tubes do not match those estimated from the experimental data, 447.

In conclusion, most of the extra-column band variance of the LC-Express Ultra system is due to the sample dispersion taking place in the injection valve, in the flow cell, and their connections with the 25 μm × 150 mm connecting tube. The contribution of the injected volume (0.160 μL) at a flow rate of 60 μL/min (0.0021 μL²) accounts for 20% of the total system variance. The contribution of a 25 μm × 150 mm PEEKSIL tube to the measured band dispersion is negligible, being smaller than 3%. As a first assumption, consider the valve and detection sensor volumes to have the same variance as ideal mixers (i.e., the square of their respective volume). The maximum peak variance would be $0.065^2 + 0.100^2 = 0.0142$ μL². In contrast, if both the valve and the detector are dispersionless, the minimum peak variance would be $0.065^2/12 + 0.10^2/12 = 0.0012$ μL². As expected, the experimental values recorded between 10 and 60 μL/min are intermediate values, between 0.0065 and 0.0101 μL².

The detection cell of the μHPLC system is 5 mm long. Thus, its radius is 40 μm. Therefore, at flow rates of 10 and 60 μL/min, Eq. 13 predicts band variances of 0.0017 and 0.0073 μL², respectively. By simple difference, we estimate the variance contribution of the injection valve at 0.0048 and 0.0028 μL², respectively.

4.2. Column contribution and performance

In the previous section, we analyzed the contributions of the different parts of the LC-Express Ultra μHPLC system to the total experimental peak variance of naphthalene at flow rates between 10 and 60 μL. The contribution (Eq. 13) of the 25 μm I.D. PEEKSIL tube inserted between the injection valve and the detection cell to the overall system band broadening (Fig. 3) was found negligible (<2%).

In the presence of the column, the 25 μm × 150 mm PEEKSIL tube is replaced by a 25 μm × 100 mm PEEKSIL tube (between the injection valve and the column) and a 25 μm × 70 mm capillary filter (between the column and the detector cell). However, the capillary filter does not affect the peak variance, because the column efficiency is nearly unchanged when replacing a 50 mm long PEEKSIL tube by the capillary filter, which is consistent with the previous results, that the connecting tubes have little effect on the system band dispersion. Fig. 4A and B compares the chromatograms of naphthalene recorded with the 0.5 mm × 50 mm Halo-C_{18} column, when using these different devices.

As a consequence, the corrections to be made for the HETP measured with the three 0.5 mm × 50 mm columns used in this work are the system peak variances measured with the 150 mm long

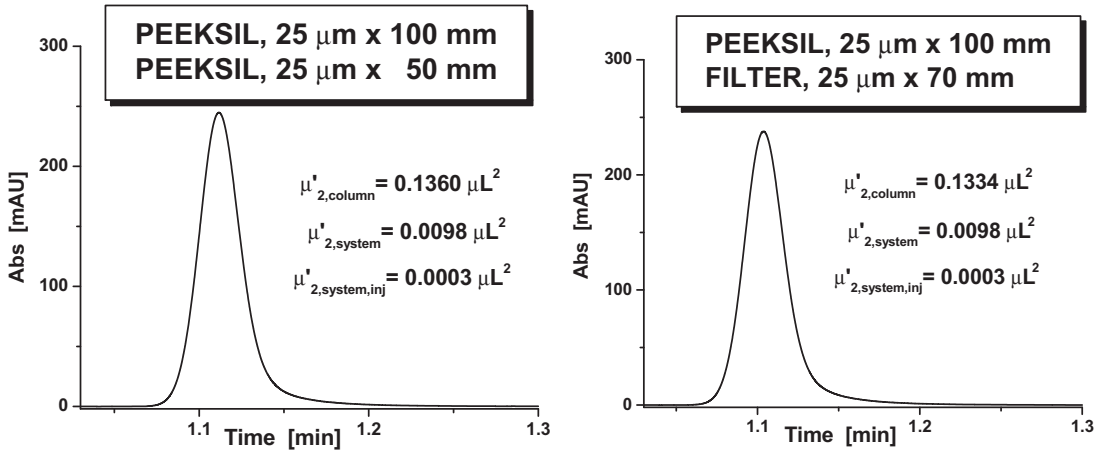

Fig. 4. Example of band profiles of naphthalene ($k = 2.3$) recorded with the LC-Express Ultra system and a 0.5 mm × 50 mm Halo-C_{18} column. Eluent: acetonitrile/water, 65/35, v/v. $T = 295$ K. Flow rate: 20 μL/min. The injection volume was fixed at 60 nL. The sampling rate was 100 Hz. **Left:** the column is connected to a 25 μm × 100 mm and 25 μm ×50 mm PEEKSIL tubes. **Right:** the column is connected to a 25 μm ×100 mm PEEKSIL tube and to a 25 μm ×70 mm capillary filter. Note the unchanged peak variance of naphthalene.

PEEKSIL tube. We now analyze the results obtained with the column packed with fully porous 3 μm particles.

4.2.1. Fully porous particles: 3 μm Prontosil-C_{18}-EP-120

The column Prontosil-C_{18}-EP-120 was packed by the instrument manufacturer. The column was used as received. Fig. 5 shows the corrected reduced plate heights (two repeats) of naphthalene measured by peak moment integration.

Strikingly, no minimum value of the reduced plate height is observed, although the smallest flow rate was 10 μL. This is unusual for retained compounds, which have a reduced B coefficient around 4.0 [36,37]. Fig. 5 shows that this is due to the high value of the apparent C coefficient of the van Deemter equation, 0.20, much larger than the typical value of 0.010 for retained compound [37], which explains the steep asymptote of the van Deemter curve. The expression of the solid-liquid mass transfer resistance coefficient is

$$C = \frac{1}{30}\frac{\epsilon_e}{1-\epsilon_e}\left(\frac{k_1}{1+k_1}\right)^2\frac{D_m}{D_p} \tag{14}$$

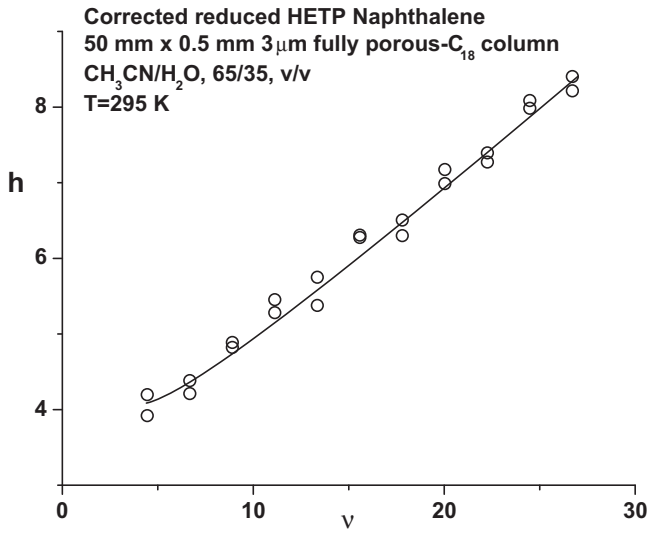

Fig. 5. Corrected reduced plate heights of naphthalene ($k = 2.8$) on the 0.5 mm × 50 mm column packed with 3 μm Prontosil-C_{18}-EP-120 fully porous particles. Eluent: acetonitrile/water, 65/35, v/v. $T = 295$ K. Note the absence of a minimum reduced plate height at flow rates between 10 and 60 μL/min.

where ϵ_e is the external porosity ($\epsilon_e \simeq 0.4$) of the packed column. For naphthalene, the zone retention factor is $k_1 \simeq 5.5$, and $D_p \simeq 1.25 D_m$ is the diffusivity of the sample across the porous particles. D_p is larger than D_m, due to the contribution of surface diffusion to the total diffusive flux of sample across the particles. Therefore, the C coefficient was expected to be around 0.012, about 15 times smaller than the experimental value. A probable explanation for this apparent contradiction is a poor packing of the column bed and a rapid increase of the eddy diffusion A term with increasing flow rate. Trans-column or at least long-range velocity biases could possibly limit the efficiency of this column.

Fig. 6A and B shows the peak profiles of naphthalene at flow rates of 10 and 60 μL/min. The significant loss of efficiency at high flow rates is not caused by some severe peak tailing but by a large peak width at half height. The reason for this problem is unknown. It might be related to difficulties in packing uniformly fine particles (3 μm) in very narrow (0.5 mm I.D.) tubes. The shear stress applied by the column wall to the particles could affect the radial homogeneity of the bed, especially for very smooth particles. The minimum reduced plate height of 4.6 mm I.D. columns packed with 3 μm particles is likely to be 2.0–2.5.

The performance of 0.5 mm I.D. columns could be improved only by minimizing the negative impact of their walls on the homogeneity of the packed beds. In the next section, we discuss the results obtained with a 0.5 mm I.D. column packed with the 2.7 μm Halo-C_{18} core–shell particles. It is assumed that the main advantage of these particles arises from their rough external surface area [4,38,10], which would restrict bed strain during bed consolidation. The large shear friction forces between core–shell particles would prevent the relative motion of the particles and this would explain why their beds are more radially homogeneous than those of fully porous particles.

4.2.2. Core–shell particles: 2.7 μm Halo-C_{18}

For the sake of assessing the repeatability of column performance, we measured the reduced plate heights of naphthalene on two distinct 0.5 mm ×50 mm columns packed with 2.7 μm Halo-C_{18} particles. Fig. 7A and B compares the performance of these two columns. A minimum reduced plate height of ca. 3.3 and 3.7 is observed on columns 1 and 2, respectively, which corresponds to efficiencies larger than that of columns packed with fully porous particles. A most striking observation is the parabolic trend of the van Deemter curve for ν larger than 12. This trend contrasts with the linear one observed for 3-C_{18}-EP-120 totally porous particles. For

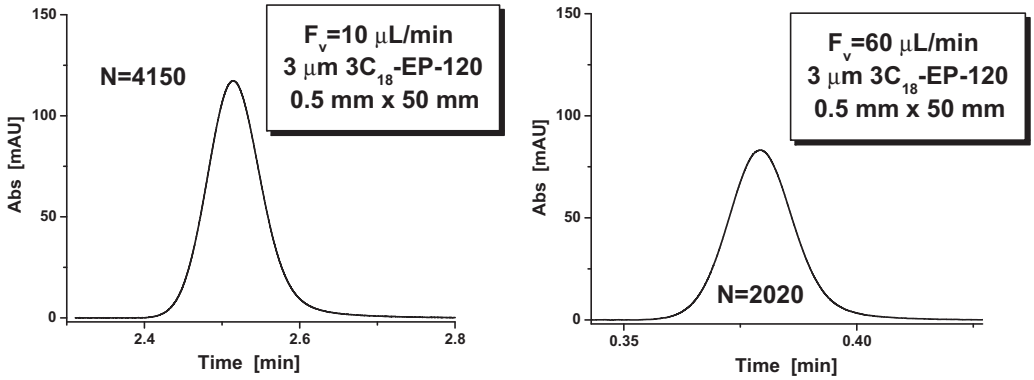

Fig. 6. Band profiles of naphthalene (k = 2.8) eluted from the LC-Express Ultra system and the 0.5 mm × 50 mm column packed with 3 μm 3-C_{18}-EP-120. The column was connected to a 25 μm ×100 mm PEEKSIL tube and to a 25 μm ×70 mm capillary filter. Eluent: acetonitrile/water, 65/35, v/v. T = 295 K. The injection volume was 160 nL. The sampling rate was 100 Hz. **Left:** flow rate 10 μL/min. **Right:** flow rate 60 μL/min. Note the significant enlargement of the half-height peak width from 10 to 60 μL/min.

ν = 25, the reduced plate heights of columns 1 and 2 become 6.5 and 7.2, corresponding to plate counts of 57 000 and 51 400 plates/m, instead of about h = 8 or 41 700 plates/m for columns packed with fully porous particles.

Could the parabolic shape of the $h(\nu)$ plot and the steep C term obtained for this column be explained by the consequences of the dissipation of the heat generated by friction of the mobile phase against the bed through which it percolates? This can easily be checked by estimating the amplitude of the radial temperature gradient (see Eq. 10) formed at a 60 μL flow rate. The maximum pressure drop was 413 × 10^5 Pa. For liquids, the average product $\overline{\alpha_p T}$ is typically around −1/3 [39]. The thermal conductivity of the bed immersed in the eluent, λ_p, was estimated at 0.48 and 0.47 W/m/K from the effective heat conductivity models of Zarichniak [40] and Jiang [41], respectively. The maximum amplitude of the radial temperature gradient would then be equal to 0.11 K only. This temperature variation is negligible and there must be some other reason for the steep C term and the parabolic curve. Most likely, as in the Prontosil column, the packed bed of Halo particles contains long-range structural defaults such as particle-arching where some particles form a local bridge, leaving large void volumes underneath, where eddy dispersion proceeds on a large scale.

Examples of peak shapes recorded with the Halo column 1 at 10 and 60 μL/min are shown in Fig. 8A and B. The relatively moderate efficiency of this column compared to those of 2.1 mm (h_{min} = 1.9) or 4.6 mm (h_{min} = 1.5) I.D. column [25] is mostly due to the significant peak tailing observed below 5% of the peak height. Had the peak be perfectly symmetrical, the fit of the experimental data to a Gaussian peak function would have generated minimum reduced plate height of 2.0 (instead of 3.3), consistent with the results measured with 2.1 mm I.D. columns.

Again, peak tailing is not due to the instrument band broadening contribution (as measured with a 25 μm ×150 mm PeekSil tube instead of a 25 μm ×100 mm PeekSil tube, the column, and the 25 μm ×70 mm capillary filter), a contribution that was systematically subtracted from the overall peak variance. The contribution of peak tailing to the peak variance at 10 μL/min is about 40% of the total peak variance, or 0.044 μL^2. The instrument band variance was only 0.008 μL^2. Therefore, peak tailing is not related to dispersion in the injection valve, the detector cell, or the connecting tubes. Surprisingly, the same observation was made for the column packed with fully porous 3 μm particles. The additional peak variance was 0.043 μL^2 at the same flow rate of 10 μL/min and a minimum reduced plate height of 2.9 instead of 4.0 should have been found. Furthermore, this peak tailing is similar for a non-retained compound and a retained one. Analysts familiar with the RPLC mode are aware that the extent of peak tailing decreases with increasing retention factor because the column variance contribution increases and the radial concentration gradients across the column diameter are more relaxed when residence time increases. That the negative effects of peak tailing persist for all compounds

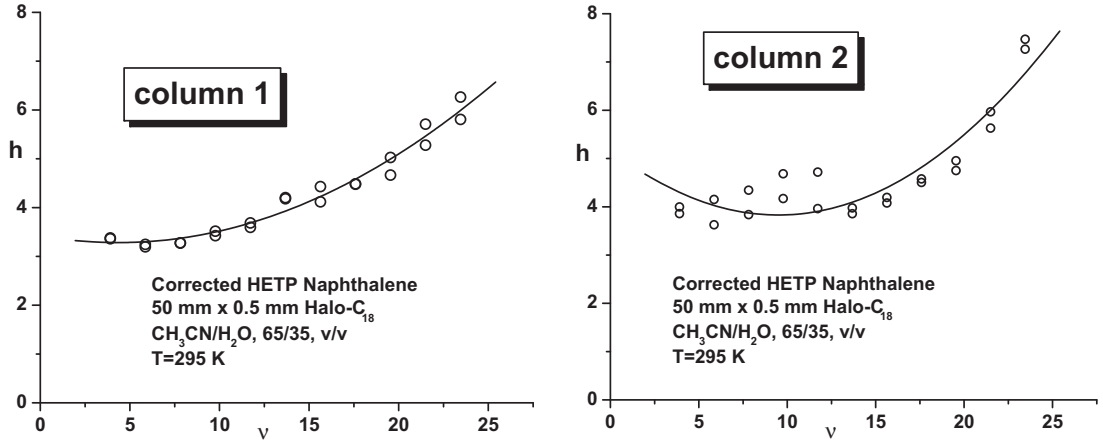

Fig. 7. Reduced plate heights of naphthalene (k = 2.3) recorded with the LC-Express Ultra system for two different 0.5 × 50 mm 2.7 μm Halo-C_{18} columns. Each column was connected to a 25 μm ×100 mm PEEKSIL tube and a 25 μm ×70 mm capillary filter. Eluent: acetonitrile/water, 65/35, v/v. T = 295 K. The injection volume was 160 nL. The sampling rate was 100 Hz. Left graph: column 1. Right graph: column 2. Note the differences and the parabolic C term.

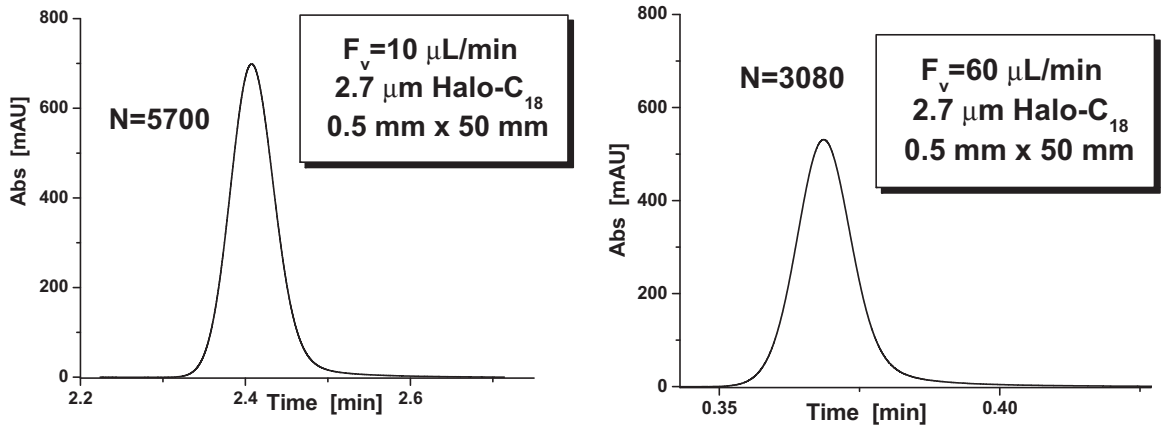

Fig. 8. Example of band profiles of naphthalene (k = 2.8) recorded with the LC-Express Ultra system and the 0.5 × 50 mm 2.7 μm Halo-C_{18} column 1. The column is connected to a 25 μm ×100 mm PEEKSIL tube and a 25 μm ×70 mm capillary filter. Eluent: acetonitrile/water, 65/35, v/v. T = 295 K. The injection volume was 160 nL. The sampling rate was 100 Hz. Left graph: the flow rate is 10 μL/min. Right graph: the flow rate is 60 μL/min. Note the significant enlargement of the half-height peak width from 10 to 60 μL/min.

(see Fig. 9), shows that they are due to band broadening taking place in the connections between the column and the connecting tubes (Peeksil and filter capillaries) and/or through the end-fitting-column assembly (frit and screw cap), which were absent during the measurement of the extra-column peak variances.

These significant dispersion phenomena were not accounted for in previous determinations of extra-column band broadening. Yet, this issue is critical in μHPLC and could become still more serious in nano-HPLC because the dispersion of bands along the column (volume ≃5 μL) and the system (volume ≃0.25 μL) is very small. If we assume h = 2 and k = 3, the variance contribution of the 0.5 × 50 mm, 2.7 μm Halo column is around 0.080 μL^2. The system (valve/connection tube/sensor detector assembly) contribution is typically 0.01 μL^2. Remarkably, the difference between the measured peak variance and that of the variance of the best-fitted Gaussian peak increases from 0.037 to 0.084 μL^2 (Halo-C_{18} column 2), from 0.040 to 0.080 μL^2 (for the 3-C_{18}-EP-120 column), and from 0.034 to 0.069 μL^2 (for Halo-C_{18} column 1) when the flow rate increases from 10 to 60 μL/min. These ranges of variations appear to be nearly independent of the nature of the packing material. This suggests that most of the decrease of the column efficiency shown in Figs. 6 and 8 with increasing flow rate is not related to an exceptionally slow solid-liquid mass transfer resistance nor to a steep eddy diffusion term.

An estimate of the intrinsic HETP of the three columns, free from all extra-column contributions, including those of the PEEKSIL/column connections and of the column enfittings/frits can be made by fitting the recorded peaks to the best Gaussian profile. Fig. 10 shows the residual reduced HETP of the three columns calculated in this way. The Gaussian function was chosen because the influence of the peak tailing observed at low fractional heights is small. Therefore, this process eliminates the contributions due to the imperfect system/column connections and column endfittings/frits to the total peak variance and provides exclusively the contribution of the highest eluted concentrations. The reduced HETPs measured from the fit of the Gaussian function to the experimental peaks show that the Halo columns 1 and 2 perform similarly, in contrast to what was observed in Fig. 7, when the numerical integrals of their first and second central moments were used to

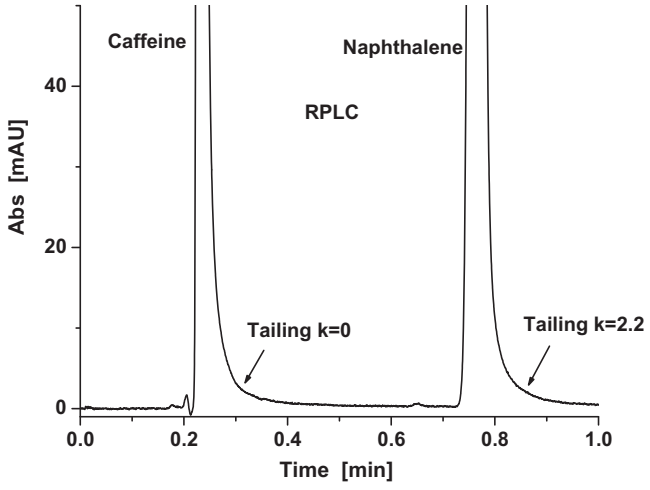

Fig. 9. Analysis of the rear peak tailing of non-retained caffeine and retained naphthalene, measured under RPLC conditions on the 0.5 mm ×50 mm Halo column 2. Flow rate: 30 μL/min. Eluent: acetonitrile/water, 65/35, v/v. T = 295 K. Note that the extent of the peak tailing is independent on the retention factor.

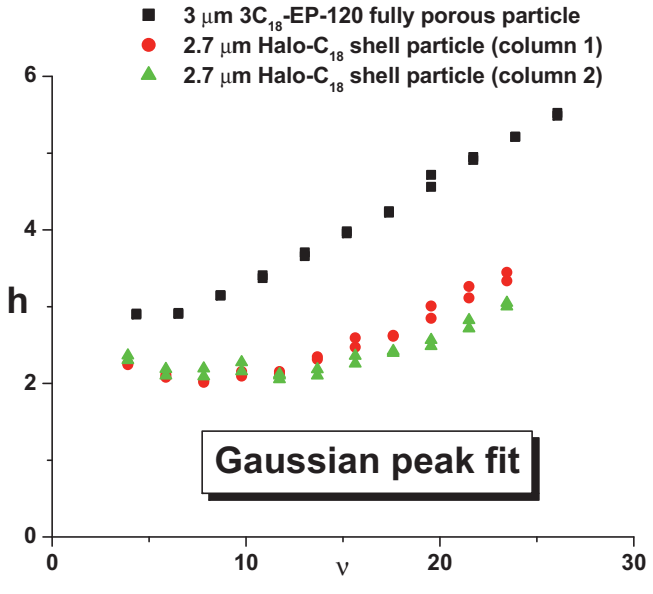

Fig. 10. Reduced plate heights of naphthalene on the three 0.5 mm ×50 mm columns, derived from the variance of the best Gaussian profiles fitted to the recorded peaks, in order to eliminate the band broadening contributed by the system/column connections and the column endfitting/frits. Eluent: acetonitrile/water, 65/35, v/v. T = 295 K.

determine the HETPs. This confirms that the contributions of the instrument and the column endfittings/frits to the total band variances are different for the two Halo columns because they are sealed with different proprietary column endfittings.

Fig. 10 confirms an important feature in column technology: rough core–shell particles are packed more uniformly in narrow-bore columns than smooth fully porous particles. This was already observed for 4.6 and 2.1 mm I.D. columns [25]. The present work extends this observation to 0.5 mm I.D. columns. The explanation could be that the high shear friction forces between rough core–shell particles limits the amplitude of the bed strain taking place during bed consolidation, resulting in a column that is more homogeneous and has a more radially uniform permeability than columns packed with smooth particles.

4.3. Perspectives with μHPLC system

This section discusses the possibility of operating 0.5 mm × 50 mm columns packed with 1 μm particles, using current μHPLC systems like the LC-Express Ultra for the analysis of low molecular weight compounds ($D_m = 1.5 \times 10^{-5}$ cm^2/s). Fully porous particles of this size have been packed in 10, 15, 30, 50, 75, 100, and 150 μm glass capillary tubes [42]. Remarkably, the minimum reduced plate heights of these columns decrease from 2.5, 2.3, 2.1, 2.0, 1.8, and 1.5 to 1.3, respectively. Scanning electron micrographs (SEM) of extruded sections of these beds show the packing arrangements of these beds to become more random with decreasing column aspect ratio, d_c/d_p. A minimum reduced plate height of 2.9 for a 500 μm I.D. column packed with 3 μm particles seems consistent with the minimum reduced HETPs of 2.5 for a 150 μm I.D. column packed with 1 μm particles. Therefore, it would be reasonable to anticipate a still larger minimum reduced plate height when packing a 0.5 mm I.D. column with 1 μm particles, possibly around 4.0. Also, the results reported in the previous two parts of this work strongly suggest that it would be better to prepare and use core–shell rather than fully porous 1 μm particles, to profit of the packing advantages conveyed by their rough external surface and obtain more uniformly packed beds. The preparation of such packing materials was recently prepared [43]. Eventually, it is reasonable to expect that columns packed with these materials could provide minimum reduced plate height of 3, corresponding to an efficiency of 16 667 plates for a 5 cm long column.

As shown in Fig. 10, the optimum reduced interstitial linear velocity is close to 10. Therefore, u_{opt} would be 1.5 cm/s and the optimum flow rate 70 μL/min. Assuming an external porosity of 40% and a Kozeny–Carman constant of 180, the specific permeability, k_0, would be 9.9×10^{-16} m^2. Thus, considering an eluent viscosity of 0.5 cP (for instance a mixture of acetonitrile and water, 80/20, v/v, at 298 K), the column back pressure would be as high as 3.8 kbar. There is still no commercial μHPLC instrument available to operate columns above 1 kbar. Two solutions are possible: (1) to reduce the column length to about 1.5 cm; or (2) to operate the column at a temperature sufficiently high that the eluent viscosity falls down to 0.15 cP, for instance the viscosity of pure acetonitrile at 140 °C. In both scenarios, the column back pressure would be reduced to 1.1 kbar, a pressure close to the one that present commercial systems can provide. Let us consider a moderately retained compound with a retention factor $k = 3$.

In the first scenario, the variance contribution of the sole chromatographic column to the peaks eluted from it would be 0.014 μL^2. At a flow rate of 70 μL/min, the extra-column variance contribution of current commercial μHPLC systems is close to 0.010 μL^2, neglecting the contributions of the Peeksil-column connectors (endfitting +frit). The present study showed that these last contributions enhance peak tailing at high flow rates, adding 0.080 μL^2 to the peak variance. Accordingly, the efficiency actually achieved ($N_{obs} = 650$) would be only 13% of the maximum expected column efficiency ($N_{theo} = 5000$) for an analysis time of 10 s. Unfortunately, this combination would present no advantage over the use, under the same conditions, of a 2.1 × 50 mm column packed with 1.7 μm particles ($N_{theo} = 16\,667$), which can provide about $N_{obs} = 9000$ plates (hence a 4 times better resolution) in about 38 s (hence in a 4 times longer analysis time), with any current VHPLC system, under nearly adiabatic conditions at a flow rate of 1.1 mL/min and for a back pressure of 1160 bar. The main advantage of micro- *versus* VHPLC separation methods is the absence of thermal effects, the heat friction generated in very narrow columns being negligible at these flow rates. Would the radial temperature gradient be fully developed, its amplitude would be 1 K and 4.7 K with 0.5 mm × 15 mm and 2.1 mm × 50 mm columns, respectively.

In the second scenario, the column length is 5 cm but the viscosity of the eluent is decreased by increasing the column temperature to about 150 °C. The effect is similar in terms of column back pressure but the efficiency provided is nine times higher than that of the 1.5 cm long column, 5580 plates, for a thrice longer analysis time (33 s). The current μHPLC systems operating 0.5 mm × 50 mm columns packed with 1 μm particles could potentially provide separation performance similar to that obtained with VHPLC systems using 2.1 mm × 50 mm columns packed with 1.7 μm particles if the band broadening contributions of the connectors between the column and the connecting tubes and/or of the dead volumes and screens inside the column could be decreased from 0.080 to about 0.030 μL^2. The advantage would then be a significant reduction of eluent consumption and the elimination of frictional heating at high flow rates. Eventually, μHPLC systems could be able to routinely use 0.5 mm and even narrower (nano-HPLC) columns packed with 1 μm shell particles if their pressure limitation was extended to a few kbar, a value already achieved in some research laboratories [42], but with a system that is most expensive, very sophisticated and not easily available to analysts.

5. Conclusion

This in-depth analysis of the performance of a commercial μHPLC system focused on its extra-column band broadening contribution. It derives the minimum dimensions of columns that could be operated without experiencing excessive performance loss. Surprisingly, when the injection valve was directly connected to the detector cell with a short tube, the system band variance was no larger than 0.012 μL^2 at the maximum flow rate of 60 μL/min. At this flow rate, most of the system variance contribution is due to the detection cell (60%), the injection valve (25%), and the injection volume of 150 nL (15%). The contributions to band dispersion of the connecting tube is negligible (<3%).

This work also compares the kinetic performance of 0.5 mm × 50 mm columns packed with either fully porous particles (Prontosil-C_{18}-EP-120 particles) or core–shell particles (2.7 μm Halo-C_{18} shell particles). Even after correction for the extra-column volume dispersion effects, the minimum reduced HETPs measured with a μHPLC instrument for these columns packed with fully porous (2.9) and shell particles (2.0) were found to be significantly larger than those measured for 4.6 mm I.D. columns (2.2 and 1.5, respectively) with conventional VHPLC instruments. The efficiencies of these columns is essentially limited by band dispersion taking place in the connections between the tubes and the column and in the endfittings and frits. This confirms that manufacturers of sub-3 μm porous or core–shell particles cannot yet pack them into 0.5 mm I.D. columns that perform as well as are the 4.6 mm I.D. columns that they routinely make.

The μHPLC instruments and narrow-bore columns might outperform current VHPLC instruments and conventional HPLC columns when instrument designers find ways to reduce the extent of band spreading caused by the connections between columns and instruments, column endfittings and frits and when they can make instruments able to operate columns at inlet pressures of several kbar. Then, the use of columns packed with 1 μm particles at high temperatures would provide faster and more efficient separations, with the additional advantage of reducing solvent consumption and eliminating efficiency losses due to frictional heating.

Acknowledgments

This work was supported in part by the cooperative agreement between the University of Tennessee and the Oak Ridge National Laboratory. We thank Khaled Mriziq and Don Arnold (Eksigent, Dublin, CA, USA) for the loan of the ExpressLC®-Ultra μHPLC instrument and of the three 0.5 mm $\times$ 50 mm columns packed sub-3 μm particles. Eksigent is part of AB SCIEX.

References

[1] J.R. Mazzeo, M.K.U.D. Neue, M. Kele, R. Plumb, Anal. Chem. 77 (2005) 460A.
[2] J.J. DeStefano, T.J. Langlois, J.J. Kirkland, J. Chromatogr. Sci. 46 (2007) 254.
[3] J.J. Kirkland, T.J. Langlois, J.J. DeStefano, Am. Lab. 39 (2007) 18.
[4] F. Gritti, G. Guiochon, J. Chromatogr. A 1157 (2007) 289.
[5] A. Cavazzini, F. Gritti, K. Kaczmarski, N. Marchetti, G. Guiochon, Anal. Chem. 79 (2007) 5972.
[6] N. Marchetti, A. Cavazzini, F. Gritti, G. Guiochon, J. Chromatogr. A 1163 (2007) 203.
[7] F. Gritti, G. Guiochon, J. Chromatogr. A 1176 (2007) 107.
[8] F. Gritti, I. Leonardis, D. Shock, P. Stevenson, A. Shalliker, G. Guiochon, J. Chromatogr. A 1217 (2010) 1589.
[9] F. Gritti, G. Guiochon, J. Chromatogr. A 1217 (2010) 1604.
[10] F. Gritti, G. Guiochon, J. Chromatogr. A 1218 (2011) 1915.
[11] S.A. Schuster, B. Wagner, B. Boyes, J. Kirkland, J. Chromatogr. Sci. 48 (2010) 566.
[12] R. Plumb, J.R. Mazzeo, E.S. Grumbach, P. Rainville, M. Jones, T. Wheat, U.D. Neue, B. Smith, K.A. Johnson, J. Sep. Sci. 30 (2007) 1158.
[13] F. Gritti, G. Guiochon, J. Chromatogr. A 1217 (2010) 7677.
[14] F. Gritti, G. Guiochon, J. Chromatogr. A 1218 (2011) 4632.
[15] F. Gritti, C.A. Sanchez, T. Farkas, G. Guiochon, J. Chromatogr. A 1217 (2010) 3000.
[16] F. Gritti, G. Guiochon, J. Chromatogr. A 1221 (2011) 2.
[17] F. Gritti, G. Guiochon, Anal. Chem. 81 (2009) 3365.
[19] F. Gritti, G. Guiochon, Anal. Chem. 80 (2008) 6488.
[20] F. Gritti, G. Guiochon, J. Chromatogr. A 1206 (2008) 113.
[21] F. Gritti, G. Guiochon, J. Chromatogr. A 1216 (2009) 1353.
[22] F. Gritti, G. Guiochon, J. Chromatogr. A 1217 (2010) 1485.
[23] F. Gritti, G. Guiochon, Chem. Eng. Sci. 65 (2010) 6310.
[24] F. Gritti, G. Guiochon, J. Chromatogr. A 1217 (2010) 5069.
[25] F. Gritti, G. Guiochon, J. Chromatogr. A 1218 (2011) 1592.
[26] J.C. Giddings, Dynamics of Chromatography, Marcel Dekker, New York, NY, 1965.
[27] H. Poppe, J. Kraak, J. Huber, H. van der Berg, Chromatographia 36 (1981) 515.
[28] H. Lin, S. Horváth, Chem. Eng. Sci. 36 (1981) 47.
[29] F. Gritti, G. Guiochon, J. Chromatogr. A 1218 (2011) 4452.
[30] H. Gao, P. Stevenson, F. Gritti, G. Guiochon, J. Chromatogr. A 1222 (2012) 81.
[31] P. Stevenson, F. Gritti, G. Guiochon, J. Chromatogr. A 1218 (2011) 8255.
[32] F. Gritti, G. Guiochon, J. Chromatogr. A 1218 (2011) 5216.
[33] R. Aris, Proc. R. Soc. A235 (1956) 67.
[34] G. Taylor, Proc. R. Soc. A219 (1953) 196.
[35] K.J. Fountain, U.D. Neue, E.S. Grumbach, D.M. Diehl, J. Chromatogr. A 1216 (2009) 5979.
[36] F. Gritti, G. Guiochon, J. Chromatogr. A, in preparation.
[37] F. Gritti, T. Farkas, J. Heng, G. Guiochon, J. Chromatogr. A 1218 (2011) 8209.
[38] F. Gritti, I. Leonardis, J. Abia, G. Guiochon, J. Chromatogr. A 1217 (2010) 3819.
[39] M. Martin, G. Guiochon, J. Chromatogr. A 1090 (2005) 16.
[40] Y. Zarichnyak, V. Novikov, Inzh. Fizi. Zh. 34 (1978) 648.
[41] F. Jiang, A. Sousa, Heat Mass Transfer 43 (2007) 479.
[42] K. Patel, A. Jerkovich, J. Link, J.W. Jorgenson, Anal. Chem. 76 (2004) 5777.
[43] L. Blue, J. Jorgenson, Anal. Chem. 83 (2011).